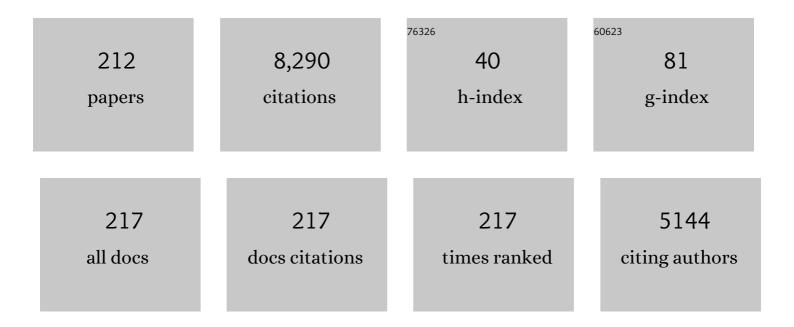
List of Publications by Year in descending order

Source: https://exaly.com/author-pdf/3782432/publications.pdf Version: 2024-02-01



НиныЦ

#	Article	IF	CITATIONS
1	Modelling and prediction of surface roughness in wire arc additive manufacturing using machine learning. Journal of Intelligent Manufacturing, 2022, 33, 1467-1482.	7.3	83
2	Hot Deformation Behavior and Recrystallization Mechanism in an As-Cast CoNi-Based Superalloy. Metals and Materials International, 2022, 28, 1488-1498.	3.4	10
3	A defect detection system for wire arc additive manufacturing using incremental learning. Journal of Industrial Information Integration, 2022, 27, 100291.	6.4	15
4	Creep properties, microstructural evolution, and fracture mechanism of an Al added high Cr ODS steel during creep deformation at 600°C. Journal of Nuclear Materials, 2022, 558, 153376.	2.7	8
5	Co-strengthening of dislocations and precipitates in alumina-forming austenitic steel with cold rolling followed by aging. Materials Science & Engineering A: Structural Materials: Properties, Microstructure and Processing, 2022, 831, 142181.	5.6	19
6	lsothermal oxidation behavior of Wâ€free Co–Ni–Alâ€based superalloy at high temperature. Materials and Corrosion - Werkstoffe Und Korrosion, 2022, 73, 513-525.	1.5	4
7	Effects of Al addition on high temperature oxidation behavior of 16Cr ODS steel. Corrosion Science, 2022, 195, 110008.	6.6	20
8	Neutron diffraction residual stress determinations in titanium aluminide component fabricated using the twin wire-arc additive manufacturing. Journal of Manufacturing Processes, 2022, 74, 141-150.	5.9	18
9	Microstructural characterization and oxidation performance of solution-annealed and precipitation hardened wire-arc additively manufactured Inconel 718 superalloys. Additive Manufacturing, 2022, 51, 102602.	3.0	3
10	Effect of microstructure on temperature dependence of deformation behavior in polycrystalline CoNi-based superalloy. Journal of Materials Science, 2022, 57, 687-699.	3.7	4
11	Evolution of Y2O3 precipitates in ODS-316ÂL steel during reactive-inspired ball-milling and spark plasma sintering processes. Powder Technology, 2022, 398, 117072.	4.2	9
12	Vision-based melt pool monitoring for wire-arc additive manufacturing using deep learning method. International Journal of Advanced Manufacturing Technology, 2022, 120, 551-562.	3.0	26
13	Towards intelligent monitoring system in wire arc additive manufacturing: a surface anomaly detector on a small dataset. International Journal of Advanced Manufacturing Technology, 2022, 120, 5225-5242.	3.0	14
14	Blackening Mechanism and Mechanical Properties Variation of Zirconia Ceramic Induced by Active Metal Brazing. Advanced Engineering Materials, 2022, 24, .	3.5	4
15	Tailoring the tempered microstructure of a novel martensitic heat resistant steel G115 through prior cold deformation and its effect on mechanical properties. Materials Science & Engineering A: Structural Materials: Properties, Microstructure and Processing, 2022, 841, 143015.	5.6	11
16	Evolution of thermally induced white etching layer at rail surface during multiple wheel/train passages. International Journal of Fatigue, 2022, 159, 106799.	5.7	17
17	On the Effect of Heat Input and Interpass Temperature on the Performance of Inconel 625 Alloy Deposited Using Wire Arc Additive Manufacturing–Cold Metal Transfer Process. Metals, 2022, 12, 46.	2.3	9
18	High-temperature creep property deterioration of the alumina-forming austenitic steel: Effect of σ phase. Materials Science & Engineering A: Structural Materials: Properties, Microstructure and Processing, 2022, 846, 143126.	5.6	15

#	Article	IF	CITATIONS
19	Influence of precipitates evolutions in δ-ferrite and austenite matrix on mechanical properties of alumina-forming austenitic steel. Materials Science & Engineering A: Structural Materials: Properties, Microstructure and Processing, 2022, 847, 143321.	5.6	12
20	Coarsening Evolution of γ′ Phase and Failure Mechanism of Co-Ni-Al-Ti-Based Superalloys During Isothermal Aging. Frontiers in Materials, 2022, 9, .	2.4	0
21	Microstructure evolution and mechanical properties of a Fe, Cr-rich multiphase Ni3Al-based superalloy during transient liquid phase bonding process. Journal of Materials Research and Technology, 2022, 19, 2837-2847.	5.8	6
22	Formation mechanism and evolution of white etching layers on different rail grades. International Journal of Fatigue, 2022, 163, 107100.	5.7	9
23	High-temperature oxidation behavior of modified 4Al alumina-forming austenitic steel: Effect of cold rolling. Journal of Materials Science and Technology, 2021, 68, 91-102.	10.7	47
24	The Correlation Between the Microstructural Parameters and Mechanical Properties of Reduced Activation Ferritic–Martensitic (RAFM) Steel: Influence of Roll Deformation and Medium Temperature Tempering. Metallurgical and Materials Transactions A: Physical Metallurgy and Materials Science, 2021, 52, 119-128.	2.2	8
25	Effect of the post-production heat treatment on phase evolution in the Fe3Ni–FeNi functionally graded material: An in-situ neutron diffraction study. Intermetallics, 2021, 129, 107032.	3.9	13
26	Enhancing the (FeMnCrNiCo + TiC) cladding layer by in-situ laser remelting. Surface Engineering, 2021, 37, 1496-1502.	2.2	8
27	OICP: An Online Fast Registration Algorithm Based on Rigid Translation Applied to Wire Arc Additive Manufacturing of Mold Repair. Materials, 2021, 14, 1563.	2.9	4
28	High-temperature oxidation performance of wire-arc additively manufactured Inconel 718 superalloys. Materials Science and Technology, 2021, 37, 413-423.	1.6	7
29	Robotic skeleton arc additive manufacturing of aluminium alloy. International Journal of Advanced Manufacturing Technology, 2021, 114, 2945-2959.	3.0	3
30	A shape control strategy for wire arc additive manufacturing of thin-walled aluminium structures with sharp corners. Journal of Manufacturing Processes, 2021, 64, 253-264.	5.9	15
31	The influence of post-weld tempering temperatures on microstructure and strength in the stir zone of friction stir welded reduced activation ferritic/martensitic steel. Materials Science & Engineering A: Structural Materials: Properties, Microstructure and Processing, 2021, 814, 141224.	5.6	10
32	Microstructure and Tensile Strength of the Bonded Interfaces and Parent Materials in W/ODS Steel Joints Fabricated by Direct SSDB. Metallurgical and Materials Transactions A: Physical Metallurgy and Materials Science, 2021, 52, 3647-3660.	2.2	5
33	A practical fabrication strategy for wire arc additive manufacturing of metallic parts with wire structures. International Journal of Advanced Manufacturing Technology, 2021, 115, 3197-3212.	3.0	13
34	The effects of multiple repair welds on a quenched and tempered steel for naval vessels. Welding in the World, Le Soudage Dans Le Monde, 2021, 65, 1997-2012.	2.5	5
35	The well-distributed volumetric heat source model for numerical simulation of wire arc additive manufacturing process. Materials Today Communications, 2021, 27, 102430.	1.9	16
36	Edge Microstructure and Strength Gradient in Thermally Cut Ti-Alloyed Martensitic Steels. Metals, 2021, 11, 1138.	2.3	0

#	Article	IF	CITATIONS
37	Influence of Al addition on the microstructure and mechanical properties of Zr-containing 9Cr-ODS steel. Journal of Materials Research and Technology, 2021, 13, 1698-1708.	5.8	8
38	Modification and characterization of the Al concentration induced precipitate in the Fe3Al-based iron aluminide fabricated using the wire-arc additive manufacturing process. Materials Characterization, 2021, 178, 111270.	4.4	10
39	Digital image correlation study on tensile properties of high strength quenched and tempered steel weld joints prepared by K-TIG and GMAW. Materials Science & Engineering A: Structural Materials: Properties, Microstructure and Processing, 2021, 827, 142033.	5.6	10
40	Effect of Cu addition on microstructure and properties of Fe–20Ni–14Cr alumina-forming austenitic steel. Intermetallics, 2021, 138, 107312.	3.9	20
41	Defects in black zirconia responsible for solar energy harvesting. Journal of Materials Chemistry C, 2021, 9, 16732-16740.	5.5	7
42	Effect of interlayer on microstructure and mechanical properties of diffusional-bonded Ni3Al-based superalloy/S31042 steel joint. Journal of Manufacturing Processes, 2021, 72, 252-261.	5.9	7
43	The Precipitated Particle Refinement in High-Cr ODS Steels by Microalloying Element Addition. Materials, 2021, 14, 7767.	2.9	5
44	Thermo-mechanical coupled finite element analysis of rolling contact fatigue and wear properties of a rail steel under different slip ratios. Tribology International, 2020, 141, 105943.	5.9	37
45	An overview on TiFe intermetallic for solid-state hydrogen storage: microstructure, hydrogenation and fabrication processes. Critical Reviews in Solid State and Materials Sciences, 2020, 45, 410-427.	12.3	64
46	Application of Multidirectional Robotic Wire Arc Additive Manufacturing Process for the Fabrication of Complex Metallic Parts. IEEE Transactions on Industrial Informatics, 2020, 16, 454-464.	11.3	38
47	In-Situ Fabrication of Titanium Iron Intermetallic Compound by the Wire Arc Additive Manufacturing Process. Metallurgical and Materials Transactions A: Physical Metallurgy and Materials Science, 2020, 51, 552-557.	2.2	6
48	Investigation of humping phenomenon for the multi-directional robotic wire and arc additive manufacturing. Robotics and Computer-Integrated Manufacturing, 2020, 63, 101916.	9.9	39
49	Enhancing tensile properties of wrought Ni-based superalloy ATI 718Plus at elevated temperature via morphology control of η phase. Materials Characterization, 2020, 169, 110547.	4.4	13
50	Cold Crack Monitoring and Localization in Welding Using Fiber Bragg Grating Sensors. IEEE Transactions on Instrumentation and Measurement, 2020, 69, 9228-9236.	4.7	21
51	Eutectic modification of Fe-enriched high-entropy alloys through minor addition of boron. Journal of Materials Science, 2020, 55, 14571-14587.	3.7	14
52	Interfacial Reaction-Induced Defect Engineering: Enhanced Visible and Near-Infrared Absorption of Wide Band Gap Metal Oxides with Abundant Oxygen Vacancies. ACS Applied Materials & Interfaces, 2020, 12, 55417-55425.	8.0	21
53	Thermal induced phase evolution of Fe–Fe3Ni functionally graded material fabricated using the wire-arc additive manufacturing process: An in-situ neutron diffraction study. Journal of Alloys and Compounds, 2020, 826, 154097.	5.5	25
54	Fabrication of FeNi intermetallic using the wire-arc additive manufacturing process: A feasibility and neutron diffraction phase characterization study. Journal of Manufacturing Processes, 2020, 57, 691-699.	5.9	19

#	Article	IF	CITATIONS
55	Study of the kinetics of austenite grain growth by dynamic Ti-rich and Nb-rich carbonitride dissolution in HSLA steel: In-situ observation and modeling. Materials Characterization, 2020, 169, 110612.	4.4	26
56	Model-free adaptive iterative learning control of melt pool width in wire arc additive manufacturing. International Journal of Advanced Manufacturing Technology, 2020, 110, 2131-2142.	3.0	28
57	The effect of isothermal aging on creep behavior of modified 2.5Al alumina-forming austenitic steel. Materials Science & Engineering A: Structural Materials: Properties, Microstructure and Processing, 2020, 797, 140219.	5.6	30
58	Effect of post-weld heat treatment on microstructure and mechanical properties of deep penetration autogenous TIG-welded dissimilar joint between creep strength enhanced ferritic steel and austenitic stainless steel. International Journal of Advanced Manufacturing Technology, 2020, 108, 3207-3229.	3.0	13
59	Characterization of Microstructure and Stress Corrosion Cracking Susceptibility in a Multi-pass Austenitic Stainless Steel Weld Joint by Narrow-Gap TIG. Metallurgical and Materials Transactions A: Physical Metallurgy and Materials Science, 2020, 51, 4549-4562.	2.2	8
60	In-situ neutron diffraction study on the high temperature thermal phase evolution of wire-arc additively manufactured Ni53Ti47 binary alloy. Journal of Alloys and Compounds, 2020, 843, 156020.	5.5	23
61	Microstructure and Mechanical Properties of 4Al Alumina-Forming Austenitic Steel after Cold-Rolling Deformation and Annealing. Materials, 2020, 13, 2767.	2.9	12
62	Influence of white etching layer on rolling contact behavior at wheel-rail interface. Friction, 2020, 8, 1178-1196.	6.4	24
63	Effects of alloying elements on microstructure and mechanical properties of Co–Ni–Al–Ti superalloy. Materials Science & Engineering A: Structural Materials: Properties, Microstructure and Processing, 2020, 779, 139139.	5.6	34
64	Wire arc additive manufacturing of Ti6AL4V using active interpass cooling. Materials and Manufacturing Processes, 2020, 35, 845-851.	4.7	31
65	An Initial Report on the Structure–Property Relationships of a High‣trength Lowâ€Alloy Steel Subjected to Advanced Thermomechanical Processing in Ferrite. Steel Research International, 2020, 91, 1900596.	1.8	0
66	Interactions between interstitial oxygen and substitutional niobium atoms in Ti–Nb–O BCC alloys: First-principles calculations. AIP Advances, 2020, 10, 025309.	1.3	4
67	Influence of Al Addition Upon the Microstructure and Mechanical Property of Dual-Phase 9Cr-ODS Steels. Metals and Materials International, 2019, 25, 168-178.	3.4	7
68	The heterogeneous microstructure of heat affect zone and its effect on creep resistance for friction stir joints on 9Cr–1.5†W heat resistant steel. Scripta Materialia, 2019, 158, 6-10.	5.2	27
69	Microstructure and mechanical properties of large-volume gradient-structure aluminium sheets fabricated by cyclic skin-pass rolling. Philosophical Magazine, 2019, 99, 2265-2284.	1.6	7
70	The Study of the Directional Sensitivity of Fiber Bragg Gratings for Acoustic Emission Measurements. IEEE Sensors Journal, 2019, 19, 6771-6777.	4.7	9
71	Flow Characteristics of a Medium–High Carbon Mn-Si-Cr Alloyed Steel at High Temperatures. Journal of Materials Engineering and Performance, 2019, 28, 5104-5115.	2.5	9
72	Enhancement of superconductivity in FeNb _x Se _{0.95} by hole carrier doping. Journal of Materials Chemistry C, 2019, 7, 10019-10027.	5.5	14

#	Article	IF	CITATIONS
73	Neutron diffraction residual stress determinations in Fe3Al based iron aluminide components fabricated using wire-arc additive manufacturing (WAAM). Additive Manufacturing, 2019, 29, 100774.	3.0	22
74	Microstructures and tensile properties of an austenitic ODS heat resistance steel. Materials Science & Engineering A: Structural Materials: Properties, Microstructure and Processing, 2019, 767, 138419.	5.6	18
75	The effect of isothermal aging on microstructure and mechanical behavior of modified 2.5Al alumina-forming austenitic steel. Materials Science & Engineering A: Structural Materials: Properties, Microstructure and Processing, 2019, 748, 161-172.	5.6	27
76	Precipitation Strengthening in Ni–Cu Alloys Fabricated Using Wire Arc Additive Manufacturing Technology. Metals, 2019, 9, 105.	2.3	19
77	Effect of Nb doping on the microstructure and superconducting properties of FeSe. Scripta Materialia, 2019, 169, 65-69.	5.2	13
78	Corrosion behavior of an Al added high-Cr ODS steel in supercritical water at 600†°C. Applied Surface Science, 2019, 480, 969-978.	6.1	20
79	Hot deformation of alumina-forming austenitic steel: EBSD study and flow behavior. Journal of Materials Science, 2019, 54, 8760-8777.	3.7	31
80	Mitigation of thermal distortion in wire arc additively manufactured Ti6Al4V part using active interpass cooling. Science and Technology of Welding and Joining, 2019, 24, 484-494.	3.1	47
81	Microstructure and Properties of Spot Welded Joints of Hot-Stamped Ultra-High Strength Steel Used for Automotive Body Structures. Metals, 2019, 9, 285.	2.3	9
82	Comparative effect of Mn/Ti solute atoms and TiC/Ni3(Al,Ti) nano-particles on work hardening behaviour in Ni Cu alloys fabricated by wire arc additive manufacturing. Materials Science & Engineering A: Structural Materials: Properties, Microstructure and Processing, 2019, 753, 262-275.	5.6	15
83	Precipitation of Carbides and Dissolution of WidmanstĀ ¤ en Structure for Enhanced Hardness in Ti2AlNb-Based Alloys. Journal of Materials Engineering and Performance, 2019, 28, 1892-1901.	2.5	4
84	Multi-criteria decision-making analysis of different non-traditional machining operations of Ti6Al4V. Soft Computing, 2019, 23, 5259-5272.	3.6	27
85	EBSD analysis and mechanical properties of alumina-forming austenitic steel during hot deformation and annealing. Materials Science & Engineering A: Structural Materials: Properties, Microstructure and Processing, 2019, 755, 106-115.	5.6	41
86	Formation mechanisms of Y–Al–O complex oxides in 9Cr-ODS steels with Al addition. Journal of Materials Science, 2019, 54, 7893-7907.	3.7	15
87	Herringbone Structure and Significantly Enhanced Hardness in W-Modified Ti2AlNb Alloys by Spark Plasma Sintering. Metals and Materials International, 2019, 25, 1000-1007.	3.4	8
88	Characterization of 14Cr ODS Steel Fabricated by Spark Plasma Sintering. Metals, 2019, 9, 200.	2.3	13
89	Effect of Heat Input on Weld Formation and Tensile Properties in Keyhole Mode TIG Welding Process. Metals, 2019, 9, 1327.	2.3	14
90	A Combination of Keyhole GTAW with a Trapezoidal Interlayer: A New Insight into Armour Steel Welding. Materials, 2019, 12, 3571.	2.9	8

#	Article	IF	CITATIONS
91	Coarsening behavior of γ′ precipitates in the γ'+γ area of a Ni3Al-based alloy. Journal of Alloys and Compounds, 2019, 771, 526-533.	5.5	86
92	Tailoring the secondary phases and mechanical properties of ODS steel by heat treatment. Journal of Materials Science and Technology, 2019, 35, 1064-1073.	10.7	32
93	Improving the weld microstructure and material properties of K-TIG welded armour steel joint using filler material. International Journal of Advanced Manufacturing Technology, 2019, 100, 1931-1944.	3.0	18
94	Helium bubble evolution and deformation of single crystal α-Fe. Journal of Materials Science, 2019, 54, 1785-1796.	3.7	8
95	In-situ neutron diffraction characterization on the phase evolution of γ-TiAl alloy during the wire-arc additive manufacturing process. Journal of Alloys and Compounds, 2019, 778, 280-287.	5.5	20
96	Microstructural characteristics and mechanical properties of friction-stir-welded modified 9Cr–1Mo steel. Journal of Materials Science, 2019, 54, 6632-6650.	3.7	13
97	Effect of annealing treatment on microstructure evolution and creep behavior of a multiphase Ni3Al-based superalloy. Materials Science & Engineering A: Structural Materials: Properties, Microstructure and Processing, 2019, 743, 623-635.	5.6	68
98	Effect of cooling rate on microstructural evolution and hardness of self-shielded arc weld deposits containing 1Âwt% aluminium. Welding in the World, Le Soudage Dans Le Monde, 2018, 62, 685-697.	2.5	2
99	Nanoporous Al sandwich foils using size effect of Al layer thickness during Cu/Al/Cu laminate rolling. Philosophical Magazine, 2018, 98, 1537-1549.	1.6	13
100	Influences of postproduction heat treatment on Fe3Al-based iron aluminide fabricated using the wire-arc additive manufacturing process. International Journal of Advanced Manufacturing Technology, 2018, 97, 335-344.	3.0	20
101	Improvement of High-Temperature Mechanical Properties of Low-Carbon RAFM Steel by MX Precipitates. Acta Metallurgica Sinica (English Letters), 2018, 31, 706-712.	2.9	31
102	Investigation into the viability of K-TIG for joining armour grade quenched and tempered steel. Journal of Manufacturing Processes, 2018, 32, 482-493.	5.9	40
103	Thermal cycling of Fe3Al based iron aluminide during the wire-arc additive manufacturing process: An in-situ neutron diffraction study. Intermetallics, 2018, 92, 101-107.	3.9	23
104	Arc Welding Processes for Additive Manufacturing: A Review. Transactions on Intelligent Welding Manufacturing, 2018, , 3-24.	0.3	87
105	Inhibition Effect of Ti on the Formation of Martensite Lath in 14Cr Oxide Dispersion Strengthened Steel. Metals, 2018, 8, 802.	2.3	6
106	Fabrication and Characterization of a Magnetized Metal-Encapsulated FBG Sensor for Structural Health Monitoring. IEEE Sensors Journal, 2018, 18, 8739-8746.	4.7	13
107	Statistical Mechanics Treatment of the Broadened Snoek Relaxation Peak in Ternary Niobium–Vanadium–Oxygen Alloys. Materials, 2018, 11, 1948.	2.9	2
108	Analysis of the Effect of Tungsten Inert Gas Welding Sequences on Residual Stress and Distortion of CFETR Vacuum Vessel Using Finite Element Simulations. Metals, 2018, 8, 912.	2.3	17

#	Article	IF	CITATIONS
109	Engineering Hierarchical Microstructures via Advanced Thermo-Mechanical Processing of a Modern HSLA Steel. Metallurgical and Materials Transactions A: Physical Metallurgy and Materials Science, 2018, 49, 6337-6350.	2.2	9
110	Deformation Mechanism of L1 ₂ â€ <i>γ</i> ′ Phase in Bimodal <i>γ</i> ″â€ <i>γ</i> ′ Precipit Hardened Inconel 718 Superalloy. Advanced Engineering Materials, 2018, 20, 1800652.	ation 3.5	7
111	Diffusion Bonding of 9Cr Martensitic/Ferritic Heat-Resistant Steels with an Electrodeposited Ni Interlayer. Metals, 2018, 8, 1012.	2.3	7
112	Anisotropy and microstructural evolutions of X70 pipeline steel during tensile deformation. Journal of Materials Research, 2018, 33, 3512-3520.	2.6	8
113	Characterization of wire arc additively manufactured titanium aluminide functionally graded material: Microstructure, mechanical properties and oxidation behaviour. Materials Science & Engineering A: Structural Materials: Properties, Microstructure and Processing, 2018, 734, 110-119.	5.6	97
114	Effects of morphology of Mg powder precursor on phase formation and superconducting properties of Mg ¹¹ B ₂ low activation superconductor. Journal of Materials Chemistry C, 2018, 6, 8069-8075.	5.5	5
115	Effects of heat accumulation on microstructure and mechanical properties of Ti6Al4V alloy deposited by wire arc additive manufacturing. Additive Manufacturing, 2018, 23, 151-160.	3.0	101
116	Hot Deformation Behavior and Microstructure Evolution of 14Cr ODS Steel. Materials, 2018, 11, 1044.	2.9	16
117	Effects of Static Recrystallization and Precipitation on Mechanical Properties of 00Cr12 Ferritic Stainless Steel. Metallurgical and Materials Transactions B: Process Metallurgy and Materials Processing Science, 2018, 49, 1560-1567.	2.1	11
118	Mechanism for the formation of Z-phase in 25Cr-20Ni-Nb-N austenitic stainless steel. Materials Letters, 2018, 233, 16-19.	2.6	26
119	Effects of Zr Addition on Strengthening Mechanisms of Al-Alloyed High-Cr ODS Steels. Materials, 2018, 11, 118.	2.9	35
120	The influence of post-production heat treatment on the multi-directional properties of nickel-aluminum bronze alloy fabricated using wire-arc additive manufacturing process. Additive Manufacturing, 2018, 23, 411-421.	3.0	53
121	A review of the wire arc additive manufacturing of metals: properties, defects and quality improvement. Journal of Manufacturing Processes, 2018, 35, 127-139.	5.9	818
122	Austenitizing Temperature Effects on the Martensitic Transformation, Microstructural Characteristics, and Mechanical Performance of Modified Ferritic Heat-Resistant Steel. Metallurgical and Materials Transactions A: Physical Metallurgy and Materials Science, 2018, 49, 3525-3538.	2.2	10
123	Inversion Calculation of the Interatomic Potentials for Ni0.75AlxMo0.25–x Alloy Employing Microscopic Phase-Field Model. Science of Advanced Materials, 2018, 10, 904-912.	0.7	2
124	Influences of deposition current and interpass temperature to the Fe3Al-based iron aluminide fabricated using wire-arc additive manufacturing process. International Journal of Advanced Manufacturing Technology, 2017, 88, 2009-2018.	3.0	60
125	Carbide dissolution and precipitation in cold-rolled type 347H austenitic heat-resistant steel. Materials Letters, 2017, 189, 70-73.	2.6	12
126	Precipitation and hot deformation behavior of austenitic heat-resistant steels: A review. Journal of Materials Science and Technology, 2017, 33, 1448-1456.	10.7	101

#	Article	IF	CITATIONS
127	Effect of hafnium addition on the microstructure and tensile properties of aluminum added high-Cr ODS steels. Journal of Alloys and Compounds, 2017, 702, 538-545.	5.5	50
128	Evolution of Al-containing phases in ODS steel by hot pressing and annealing. Powder Technology, 2017, 311, 449-455.	4.2	19
129	Enhancement of tensile properties due to microstructure optimization in ODS steels by zirconium addition. Fusion Engineering and Design, 2017, 125, 402-406.	1.9	34
130	Laves phase precipitation behavior in the simulated fine-grained heat-affected zone of creep strength enhanced ferritic steel P92 and its role in creep void nucleation and growth. Welding in the World, Le Soudage Dans Le Monde, 2017, 61, 231-239.	2.5	11
131	Study on microstructural evolution and constitutive modeling for hot deformation behavior of a low-carbon RAFM steel. Journal of Materials Research, 2017, 32, 1376-1385.	2.6	18
132	Innovative analysis of Luders band behaviour in X80 pipeline steel. Materials Science & Engineering A: Structural Materials: Properties, Microstructure and Processing, 2017, 683, 123-128.	5.6	27
133	Microstructure and tensile properties of a 14Cr ODS ferritic steel. Materials Science & Engineering A: Structural Materials: Properties, Microstructure and Processing, 2017, 680, 347-350.	5.6	33
134	Hot deformation behavior and microstructural evolution of Nb–V–Ti microalloyed ultra-high strength steel. Journal of Materials Research, 2017, 32, 3777-3787.	2.6	13
135	Fabrication of Copper-Rich Cu-Al Alloy Using the Wire-Arc Additive Manufacturing Process. Metallurgical and Materials Transactions B: Process Metallurgy and Materials Processing Science, 2017, 48, 3143-3151.	2.1	61
136	Enhanced materials performance of Al/Ti/Al laminate sheets subjected to cryogenic roll bonding. Journal of Materials Research, 2017, 32, 3761-3768.	2.6	21
137	Precipitates and Particles Coarsening of 9Cr–1.7W–0.4Mo–Co Ferritic Heat-Resistant Steel after Isothermal Aging. Scientific Reports, 2017, 7, 5859.	3.3	24
138	Effects of heat accumulation on the arc characteristics and metal transfer behavior in Wire Arc Additive Manufacturing of Ti6Al4V. Journal of Materials Processing Technology, 2017, 250, 304-312.	6.3	217
139	Formation of Fine B2/βÂ+ÂO Structure and Enhancement of Hardness in the Aged Ti2AlNb-Based Alloys Prepared by Spark Plasma Sintering. Metallurgical and Materials Transactions A: Physical Metallurgy and Materials Science, 2017, 48, 4365-4371.	2.2	18
140	Enhancement of grain connectivity and critical current density in the ex-situ sintered MgB2 superconductors by doping minor Cu. Journal of Alloys and Compounds, 2017, 727, 1105-1109.	5.5	15
141	Enhancement of synthesis efficiency and critical current density in glycine-doped MgB2 bulks by two-step sintering. Journal of Materials Science: Materials in Electronics, 2017, 28, 5645-5651.	2.2	2
142	Microstructure characteristic and mechanical property of transformable 9Cr-ODS steel fabricated by spark plasma sintering. Materials and Design, 2017, 132, 158-169.	7.0	59
143	Rapid hydrothermal synthesis of Li3VO4 with different favored facets. Journal of Solid State Electrochemistry, 2017, 21, 2547-2553.	2.5	8
144	Austenite to polygonal-ferrite transformation and carbide precipitation in high strength low alloy steel. International Journal of Materials Research, 2017, 108, 12-19.	0.3	2

#	Article	IF	CITATIONS
145	Doping-Induced Isotopic Mg11B2 Bulk Superconductor for Fusion Application. Energies, 2017, 10, 409.	3.1	7
146	The Effect of Precipitate Evolution on Austenite Grain Growth in RAFM Steel. Materials, 2017, 10, 1017.	2.9	25
147	Enhancement of Thermal Stability and Cycling Performance of Lithium-Ion Battery at High Temperature by Nano-ppy/OMMT-Coated Separator. Journal of Nanomaterials, 2017, 2017, 1-10.	2.7	7
148	A Fiber-Coupled Self-Mixing Laser Diode for the Measurement of Young's Modulus. Sensors, 2016, 16, 928.	3.8	16
149	Fabricating Superior NiAl Bronze Components through Wire Arc Additive Manufacturing. Materials, 2016, 9, 652.	2.9	135
150	Correlation between Zn-Rich Phase and Corrosion/Oxidation Behavior of Sn–8Zn–3Bi Alloy. Metals, 2016, 6, 175.	2.3	2
151	Transverse and z-Direction CVN Impact Tests of X65 Line Pipe Steels of Two Centerline Segregation Ratings. Metallurgical and Materials Transactions A: Physical Metallurgy and Materials Science, 2016, 47, 3919-3932.	2.2	7
152	Special Rolling Techniques for Improvement of Mechanical Properties of Ultrafineâ€Grained Metal Sheets: a Review. Advanced Engineering Materials, 2016, 18, 754-769.	3.5	57
153	Superstrength of nanograined steel with nanoscale intermetallic precipitates transformed from shock-compressed martensitic steel. Scientific Reports, 2016, 6, 36810.	3.3	12
154	Mechanical properties of T23 steel welded joints without post-weld heat treatment for fossil fired boilers. Journal of Materials Research, 2016, 31, 4000-4008.	2.6	7
155	Microstructure evolution of accumulative roll bonding processed pure aluminum during cryorolling. Journal of Materials Research, 2016, 31, 797-805.	2.6	16
156	In-depth study of the mechanical properties for Fe3Al based iron aluminide fabricated using the wire-arc additive manufacturing process. Materials Science & Engineering A: Structural Materials: Properties, Microstructure and Processing, 2016, 669, 118-126.	5.6	65
157	Evaluation of quenching-induced lattice strain and superconducting properties in un-doped and glycine-doped MgB2 bulks. Journal of Materials Science: Materials in Electronics, 2016, 27, 9431-9436.	2.2	3
158	Enhanced mechanical properties of ARB-processed aluminum alloy 6061 sheets by subsequent asymmetric cryorolling and ageing. Materials Science & Engineering A: Structural Materials: Properties, Microstructure and Processing, 2016, 674, 256-261.	5.6	54
159	Hot deformation behavior of Ti–22Al–25Nb alloy by processing maps and kinetic analysis. Journal of Materials Research, 2016, 31, 1764-1772.	2.6	18
160	Adaptive path planning for wire-feed additive manufacturing using medial axis transformation. Journal of Cleaner Production, 2016, 133, 942-952.	9.3	113
161	Effects of tantalum content on the microstructure and mechanical properties of low-carbon RAFM steel. Journal of Nuclear Materials, 2016, 479, 295-301.	2.7	41
162	Fibre optic acoustic emission sensor system for hydrogen induced cold crack monitoring in welding applications. , 2016, , .		4

10

#	Article	IF	CITATIONS
163	Fibre optic acoustic emission measurement technique for crack activity monitoring in civil engineering applications. , 2016, , .		3
164	Simultaneous Grain Growth and Grain Refinement in Bulk Ultrafine-Grained Copper under Tensile Deformation at Room Temperature. Metallurgical and Materials Transactions A: Physical Metallurgy and Materials Science, 2016, 47, 3785-3789.	2.2	13
165	Thermodynamic and kinetic evidence for MgO formation and pinning behavior in glycine-doped MgB2 bulks. Journal of Materials Science, 2016, 51, 2665-2676.	3.7	4
166	The effect of postproduction heat treatment on γ-TiAl alloys produced by the GTAW-based additive manufacturing process. Materials Science & Engineering A: Structural Materials: Properties, Microstructure and Processing, 2016, 657, 86-95.	5.6	71
167	Fabrication of Fe-FeAl Functionally Graded Material Using the Wire-Arc Additive Manufacturing Process. Metallurgical and Materials Transactions B: Process Metallurgy and Materials Processing Science, 2016, 47, 763-772.	2.1	116
168	Acicular ferrite formation during isothermal holding in HSLA steel. Journal of Materials Science, 2016, 51, 3555-3563.	3.7	20
169	Towards an automated robotic arc-welding-based additive manufacturing system from CAD to finished part. CAD Computer Aided Design, 2016, 73, 66-75.	2.7	138
170	Bead modelling and implementation of adaptive MAT path in wire and arc additive manufacturing. Robotics and Computer-Integrated Manufacturing, 2016, 39, 32-42.	9.9	174
171	Automatic multi-direction slicing algorithms for wire based additive manufacturing. Robotics and Computer-Integrated Manufacturing, 2016, 37, 139-150.	9.9	127
172	Precipitation behavior of type 347H heat-resistant austenitic steel during long-term high-temperature aging. Journal of Materials Research, 2015, 30, 3642-3652.	2.6	22
173	Weld Haz Properties in Modern High Strength Niobium Pipeline Steels. , 2015, , 453-457.		2
174	Preâ€Blast Strengthening of Fe–18Mn–0.6C–1.5Al TWIP Steel. Steel Research International, 2015, 86, 760-765.	1.8	1
175	Edgeâ€Hydroxylated Boron Nitride Nanosheets as an Effective Additive to Improve the Thermal Response of Hydrogels. Advanced Materials, 2015, 27, 7196-7203.	21.0	227
176	Post-Deformation Microstructure and Texture Characterization of Fe-18Mn-0.6C-1.5Al TWIP Steel. Steel Research International, 2015, 86, 1461-1468.	1.8	3
177	Phase Transformation Behavior and Microstructural Control of High-Cr Martensitic/Ferritic Heat-resistant Steels for Power and Nuclear Plants: A Review. Journal of Materials Science and Technology, 2015, 31, 235-242.	10.7	134
178	Hydrogels: Edgeâ€Hydroxylated Boron Nitride Nanosheets as an Effective Additive to Improve the Thermal Response of Hydrogels (Adv. Mater. 44/2015). Advanced Materials, 2015, 27, 7247-7247.	21.0	8
179	Process planning for robotic wire and arc additive manufacturing. , 2015, , .		28
180	Rapid synthesis of α-Fe2O3/rGO nanocomposites by microwave autoclave as superior anodes for sodium-ion batteries. Journal of Power Sources, 2015, 280, 107-113.	7.8	123

#	Article	IF	CITATIONS
181	A practical path planning methodology for wire and arc additive manufacturing of thin-walled structures. Robotics and Computer-Integrated Manufacturing, 2015, 34, 8-19.	9.9	223
182	Fabrication of iron-rich Fe–Al intermetallics using the wire-arc additive manufacturing process. Additive Manufacturing, 2015, 7, 20-26.	3.0	82
183	Wire-feed additive manufacturing of metal components: technologies, developments and future interests. International Journal of Advanced Manufacturing Technology, 2015, 81, 465-481.	3.0	1,007
184	Effect of interpass temperature on in-situ alloying and additive manufacturing of titanium aluminides using gas tungsten arc welding. Additive Manufacturing, 2015, 8, 71-77.	3.0	70
185	Morphology and structure evolution of Y2O3 nanoparticles in ODS steel powders during mechanical alloying and annealing. Advanced Powder Technology, 2015, 26, 1578-1582.	4.1	29
186	Effect of Austenitizing Temperature on the Bainitic Transformation in a High-Carbon High-Silicon Steel. Metal Science and Heat Treatment, 2015, 57, 156-160.	0.6	6
187	Preparation and Characterization of Fe ₃ O ₄ @nSiO ₂ @mSiO ₂ –NH ₂ Core–Shell Microspheres for Extracting Allura Red from Aqueous Solution. Nano, 2015, 10, 1550122.	1.0	2
188	Influence of Heat Input on Microstructure and Toughness Properties in Simulated CGHAZ of X80 Steel Manufactured Using High-Temperature Processing. Metallurgical and Materials Transactions A: Physical Metallurgy and Materials Science, 2015, 46, 5467-5475.	2.2	24
189	Influence of aging on shape memory effect and corrosion resistance of a new Fe–Mn–Si-based alloy. Journal of Materials Research, 2015, 30, 179-185.	2.6	5
190	Simple low-temperature chemical bath route to synthesize novel Ga-doped ZnO nanostructures for high photoresponse. Journal of Materials Science: Materials in Electronics, 2015, 26, 671-676.	2.2	1
191	The formation of nano-layered grains and their enhanced superconducting transition temperature in Mg-doped FeSe0.9 bulks. Scientific Reports, 2015, 4, 6481.	3.3	9
192	A multi-bead overlapping model for robotic wire and arc additive manufacturing (WAAM). Robotics and Computer-Integrated Manufacturing, 2015, 31, 101-110.	9.9	345
193	Feasibility Study of Low Force Robotic Friction Stir Process and its Effect On Cavitation Erosion and Electrochemical Corrosion for Ni Al Bronze Alloys. Metallurgical and Materials Transactions B: Process Metallurgy and Materials Processing Science, 2014, 45, 2291-2298.	2.1	10
194	Martensitic Phase Transformation and Deformation Behavior of Fe–Mn–C–Al Twinningâ€Induced Plasticity Steel during Highâ€Pressure Torsion. Advanced Engineering Materials, 2014, 16, 927-932.	3.5	12
195	Effects of aging on shape memory and wear resistance of a Fe–Mn–Si-based alloy. Journal of Materials Research, 2014, 29, 2809-2816.	2.6	11
196	Effects of wire feed conditions on in situ alloying and additive layer manufacturing of titanium aluminides using gas tungsten arc welding. Journal of Materials Research, 2014, 29, 2066-2071.	2.6	37
197	Observations on the Zirconium Hydride Precipitation and Distribution in Zircaloy-4. Metallurgical and Materials Transactions B: Process Metallurgy and Materials Processing Science, 2014, 45, 532-539.	2.1	14
198	Development of ferrite/bainite bands and study of bainite transformation retardation in HSLA steel during continuous cooling. Metals and Materials International, 2014, 20, 19-25.	3.4	21

#	Article	IF	CITATIONS
199	Characterization of In-Situ Alloyed and Additively Manufactured Titanium Aluminides. Metallurgical and Materials Transactions B: Process Metallurgy and Materials Processing Science, 2014, 45, 2299-2303.	2.1	46
200	A tool-path generation strategy for wire and arc additive manufacturing. International Journal of Advanced Manufacturing Technology, 2014, 73, 173-183.	3.0	227
201	The Effect of Chemical Composition on Microstructure and Properties of Intercritically Reheated Coarse-Grained Heat-Affected Zone in X70 Steels. Metallurgical and Materials Transactions B: Process Metallurgy and Materials Processing Science, 2014, 45, 229-235.	2.1	25
202	Effect of inter-critically reheating temperature on microstructure and properties of simulated inter-critically reheated coarse grained heat affected zone in X70 steel. Materials Science & Engineering A: Structural Materials: Properties, Microstructure and Processing, 2014, 605, 8-13.	5.6	36
203	Influence of annealing temperature on the structural and optical properties of Mg–Al co-doped ZnO thin films prepared via sol–gel method. Ceramics International, 2014, 40, 5873-5880.	4.8	55
204	A deformation mechanism of hard metal surrounded by soft metal during roll forming. Scientific Reports, 2014, 4, 5017.	3.3	51
205	Microstructure and interface evolution of Sn-2.5Bi-1.4In-1Zn-0.3Ag/Cu joint during isothermal aging. Journal of Materials Science: Materials in Electronics, 2013, 24, 4122-4128.	2.2	3
206	Polypyrrole-coated $\hat{1}$ ±-LiFeO2 nanocomposite with enhanced electrochemical properties for lithium-ion batteries. Electrochimica Acta, 2013, 108, 820-826.	5.2	40
207	Variation of pinning mechanism and enhancement of critical current density in MgB2 bulk containing self-generated coherent MgB4 impurity. Applied Physics Letters, 2013, 103, .	3.3	19
208	Precipitation kinetics of M ₂₃ C ₆ in T/P92 heat-resistant steel by applying soft-impingement correction. Journal of Materials Research, 2013, 28, 1529-1537.	2.6	12
209	Microstructure evolution and martensitic transformation behaviors of 9Cr–1.8W–0.3Mo ferritic heat-resistant steel during quenching and partitioning treatment. Journal of Materials Research, 2013, 28, 2835-2843.	2.6	11
210	On the Compression Behavior of an Austenitic Fe–18 <scp>M</scp> n–0.6 <scp>C</scp> –1.5 <scp>A</scp> I Twinningâ€ <scp>I</scp> nduced Plasticity Steel. Steel Research International, 2013, 84, 1281-1287.	1.8	6
211	Microstructural Characterization of P91 Steel in the Virgin, Service Exposed and Postâ€Service Reâ€Normalized Conditions. Steel Research International, 2013, 84, 1302-1308.	1.8	26
212	From Single Grains to Texture. Advanced Engineering Materials, 2009, 11, 771-773.	3.5	21